Chlorine-35/37 NMR Spectroscopy of Solid Amino Acid Hydrochlorides: Refinement of Hydrogen-Bonded Proton Positions Using Experiment and Theory

David L. Bryce* and Gregory D. Sward

Department of Chemistry and Centre for Catalysis Research and Innovation, University of Ottawa, Ottawa, Ontario K1N 6N5, Canada

Received: September 8, 2006; In Final Form: October 17, 2006

Trends in the chlorine chemical shift (CS) tensors of amino acid hydrochlorides are investigated in the context of new data obtained at 21.1 T and extensive quantum chemical calculations. The analysis of chlorine-35/37 NMR spectra of solid L-tryptophan hydrochloride obtained at two magnetic field strengths yields the chlorine electric field gradient (EFG) and CS tensors, and their relative orientations. The chlorine CS tensor is also determined for the first time for DL-arginine hydrochloride monohydrate. The drastic influence of ^{1}H decoupling at 21.1 T on the spectral features of salts with particularly small ^{35}Cl quadrupolar coupling constants (C_Q) is demonstrated. The chlorine CS tensor spans (Ω) of hydrochloride salts of hydrophobic amino acids are found to be larger than those for salts of hydrophilic amino acids. A new combined experimental−theoretical procedure is described in which quantum chemical geometry optimizations of hydrogen-bonded proton positions around the chloride ions in a series of amino acid hydrochlorides are cross-validated against the experimental chlorine EFG and CS tensor data. The conclusion is reached that the relatively computationally inexpensive B3LYP/3-21G* method provides proton positions which are suitable for subsequent higher-level calculations of the chlorine EFG tensors. The computed value of Ω is less sensitive to the proton positions. Following this cross-validation procedure, $|C_Q(^{35}\mathrm{Cl})|$ is generally predicted within 15% of the experimental value for a range of HCl salts. The results suggest the applicability of chlorine NMR interaction tensors in the refinement of proton positions in structurally similar compounds, e.g., chloride ion channels, for which neutron diffraction data are unavailable.

Introduction

The availability of high-field solid-state nuclear magnetic resonance (NMR) spectrometers, e.g., those with ^{1}H resonance frequencies of 800 MHz, 900 MHz, and above, has created new opportunities for the study of quadrupolar nuclei ($I > 1/2$) with low resonance frequencies or large quadrupole moments, and for nuclei with both of these properties. For example, Stebbins et al. have described applications of 18.8 and 21.1 T solid-state ^{27}Al, ^{17}O, ^{39}K, and ^{35}Cl NMR spectroscopy to study oxide materials.[1−3] Gan et al. used magnetic fields as high as 40 T to achieve chemical shift resolution between four different aluminum environments in aluminoborate.[4] Ellis and colleagues have applied high-field ^{67}Zn NMR at low temperature to study zinc binding environments of biological relevance.[5,6,7,8] Magic-angle-spinning (MAS) NMR in a magnetic field of 19.6 T has been applied by Wu and co-workers to detect potassium cations in guanine-quadruplex structures[9] as well as to explore cation−π interactions in alkali metal tetraphenylborates.[10] Cross and co-workers have demonstrated the utility of ^{17}O solid-state NMR at 21.1 T for characterizing the ion channel gramicidin.[11,12] The major reason that higher fields are so beneficial for the study of quadrupolar nuclei in the solid state is the inverse scaling of the second-order quadrupolar broadening of the central transition (CT) with the strength of the applied magnetic field, B_0. The high magnetic fields therefore lead to narrower lines and an overall increase in sensitivity.

Our own recent work has raised the possibility of applying ultrahigh field chlorine-35/37 solid-state NMR spectroscopy[13] as a probe of ion binding environment in chloride ion channels.[14] In this work, the chlorine electric field gradient (EFG) and chemical shift (CS) tensors for a variety of amino acid hydrochlorides with chloride ion binding environments representative of those in the ClC ion channels were characterized. Gervais et al. have also recently presented a solid-state multinuclear magnetic resonance study of several amino acids and their hydrochloride salts, including some ^{35}Cl NMR studies.[15] In the present work, trends in the magnitude of the chlorine chemical shift tensor are elucidated in the context of new experimental data for L-tryptophan hydrochloride (see Figure 1) and DL-arginine hydrochloride monohydrate. Interactions between tryptophan moieties and chloride ions are of direct biological importance as illustrated, for example, by a recent publication which suggests a mechanism for the electrophilic addition of chloride to tryptophan by the PrnA enzyme.[16] Furthermore, interactions between chloride and various amino acid sidechains are responsible for chloride ion selectivity and transport in various ion channels including the ClC type.[17−20] The present study provides new insights into how the local chloride binding environment is manifested in the chlorine CS tensor.

Another major thrust of the present work is to determine how sensitive the chlorine EFG and nuclear magnetic shielding tensors are to the local molecular structure surrounding the chloride ions, specifically the positions of the protons to which they are hydrogen-bonded. Ashbrook and Duer have recently described in detail how structural information may be extracted from solid-state NMR experiments performed on quadrupolar nuclei.[21] Motivated by their review, we present here a new cross-

* Author to whom correspondence should be addressed. E-mail dbryce@uottawa.ca. phone 613-562-5800 ext 2018. fax 613-562-5170.

10.1021/jp065878c CCC: $33.50
Published on Web 12/07/2006

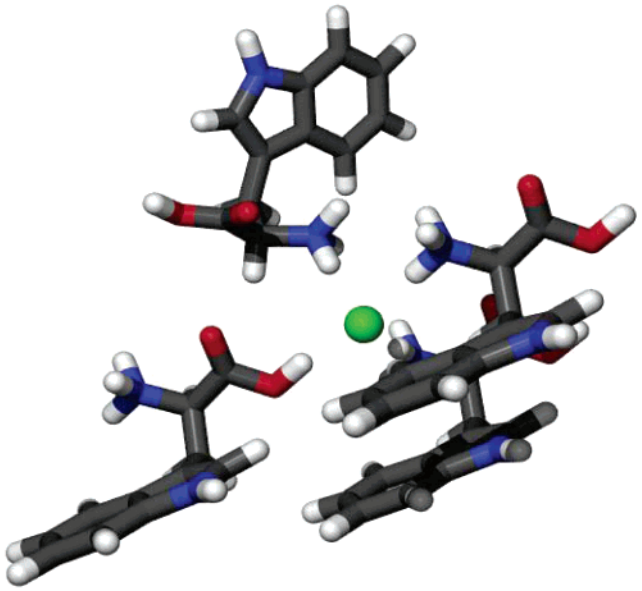

Figure 1. Environment around the chloride anion in solid L-tryptophan hydrochloride according to the X-ray diffraction analysis of Takigawa et al.[40] This is the model used for quantum chemical calculations in the present work, consisting of one chloride ion and four tryptophan moieties. The chloride ion forms hydrogen bonds with three NH_3^+ groups and with one OH group. Chlorine is shown in green, carbon in gray, nitrogen in blue, oxygen in red, and hydrogen in white.

validation approach to determine the quality of quantum chemically optimized hydrogen-bonded proton positions, which uses the experimental chlorine quadrupolar coupling data.

Background Theory

The theory relevant to solid-state NMR spectroscopy of a half-integer spin quadrupolar nucleus with an anisotropic chemical shift tensor under the high-field approximation has been presented several times.[22−24] We present here only the conventions used in the current work. The two most important interactions to consider presently are the nuclear magnetic shielding interaction and the quadrupolar interaction.

Since the nuclear magnetic shielding tensor (σ) cannot be measured directly in an NMR experiment, one measures the chemical shift tensor (δ). In its principal axis system (PAS), the CS tensor magnitude is characterized by three principal components, $\delta_{11} \geq \delta_{22} \geq \delta_{33}$. The isotropic chemical shift (δ_{iso}), span (Ω), and skew (κ) offer alternative representations of the magnitude of the CS tensor:[25]

$$\delta_{iso} = \frac{(\delta_{11} + \delta_{22} + \delta_{33})}{3} \tag{1}$$

$$\Omega = \delta_{11} - \delta_{33} \tag{2}$$

$$\kappa = \frac{3(\delta_{22} - \delta_{iso})}{\Omega} \tag{3}$$

To compare experimental chemical shifts with calculated magnetic shielding constants from quantum chemistry, the value of the isotropic shielding constant of the reference compound, σ_{iso}(ref), must be known:

$$\delta_{iso} = \frac{\sigma_{iso}(\text{ref}) - \sigma_{iso}}{1 - \sigma_{iso}(\text{ref})} \approx \sigma_{iso}(\text{ref}) - \sigma_{iso} \tag{4}$$

where the second equality is valid for most light elements since magnetic shielding constants are on the order of 10^{-6}. The value of σ_{iso}(ref) is known to be 974 ppm for chlorine nuclei in an infinitely dilute aqueous NaCl solution.[26]

The NMR spectra of ^{35}Cl (N.A. = 75.53%) and ^{37}Cl (N.A. = 24.47%), both with nuclear spin quantum numbers of 3/2, are also affected by the nuclear quadrupolar interaction between their nuclear electric quadrupole moment (Q) and the surrounding EFG tensor. For the chlorine solid-state NMR spectra presented in this work, only the central transition (CT, 1/2 ↔ -1/2) is observed. All experiments were performed within the regime of the high-field approximation, where the Larmor frequency (ν_L) is much greater than the quadrupolar frequency, $\nu_Q = 3C_Q/(2I(2I - 1))$.

In its PAS, the EFG tensor is characterized by three eigenvalues: $|V_{33}| \geq |V_{22}| \geq |V_{11}|$. The quadrupolar coupling constant, C_Q, is related to the principal component of largest magnitude as follows:

$$C_Q = \frac{eV_{33}Q}{h} \tag{5}$$

where e is the charge on an electron, h is Planck's constant, and Q is the nuclear electric quadrupole moment. The asymmetry parameter of the EFG tensor is given by:

$$\eta_Q = \frac{V_{11} - V_{22}}{V_{33}} \tag{6}$$

In addition to the EFG and CS tensor magnitudes, the relative orientation of these two tensors, as described by three Euler angles (α, β, γ), is also available experimentally. These angles define the counter-clockwise rotations required to bring the EFG PAS into coincidence with the CS PAS. We follow the convention where α describes the initial counter-clockwise rotation about the z-axis of the coordinate system, β is the subsequent rotation about the y-axis of the new coordinate system, and γ is the final rotation around the new z-axis.

Experimental Section

(i) Sample Preparation. L-Glutamic acid hydrochloride and DL-arginine hydrochloride monohydrate were purchased from Aldrich and used as received. L-tryptophan hydrochloride and L-lysine hydrochloride were prepared by dissolving the corresponding amino acid (Aldrich) in a hot solution of hydrochloric acid, followed by filtering of the resulting HCl salt. The decomposition point of L-tryptophan hydrochloride was measured to be 240−245 °C using a Barnstead/Electrothermal MelTemp melting point apparatus. Additional sample characterization details for selected amino acid hydrochlorides have been reported previously.[14] Samples were ground into fine powders and packed into zirconia rotors for solid-state NMR experiments.

(ii) NMR Spectroscopy. Chlorine-35/37 NMR experiments were performed on a 500 MHz (B_0 = 11.75 T) Bruker Avance spectrometer at the University of Ottawa, and on a 900 MHz (B_0 = 21.1 T) Bruker Avance II spectrometer at the National Ultrahigh-Field NMR Facility for Solids in Ottawa. Experiments were carried out at ambient temperature. No corrections were made for potential effects of sample heating under fast MAS conditions.

For experiments at 11.75 T, a 4 mm Bruker HX probe tuned to 49.00 MHz (^{35}Cl) or 40.79 MHz (^{37}Cl) was used. For ^{35}Cl, the $\pi/2$ pulse length was determined to be 4.4 μs using a sample of powdered NaCl. The 'solid' CT $\pi/2$ pulse used for amino acid hydrochlorides was therefore 2.2 μs. Chemical shifts were

referenced with respect to solid NaCl. A hyperbolic secant spin−echo sequence,[27,28] with high-power proton decoupling during acquisition, was used.

A Bruker MAS DVT 3.2 HX probe (serial number 0001) was employed for experiments at 21.1 T. The X channel was tuned to 88.2 MHz for ^{35}Cl. A solid $\pi/2$ pulse length of 1.62 μs was determined using solid NaCl as a setup sample. Chemical shifts were referenced with respect to solid NaCl. Proton decoupling (114 kHz) was applied during acquisition. MAS rates ranging from 17 to 22 kHz were typically used. Spectra were acquired using a single pulse with proton decoupling or using a spin−echo with proton decoupling. The quadrupolar Carr−Purcell−Meiboom−Gill (QCPMG) experiments[29,30,31,32] used a train of 17 π pulses with a spacing of 220 μs between them (following the initial $\pi/2$ pulse), resulting in an acquisition time of 3.74 ms and a spacing of 4545 Hz between spikelets in the Fourier-transformed spectrum. A home-built (J. Bennett, National Research Council, Ottawa) single-channel 5 mm solenoid probe (version #1) was also used for some experiments. The solid $\pi/2$ pulse was determined to be 3.0 μs on this probe. Recycle delays were typically 1 to 5 s.

(iii) Data Processing and Simulations. NMR spectra were processed using XWinNMR 3.2 or TopSpin 1.3. Gaussian apodization and zero-filling of the FID to at least twice the original size were performed prior to Fourier transformation. Left-shifting was applied as appropriate to FIDs acquired with a spin−echo pulse sequence.

NMR spectra were simulated using the WSOLIDS software package,[33] which incorporates the space-tiling algorithm of Grant and co-workers.[34] Some spectra of MAS samples were also simulated using SIMPSON.[35] The large zcw317810 crystal file was used for powder averaging in SIMPSON.[36] Spectral stack plots were generated using DMFit.[37]

In order to maximize the accuracy and precision with which EFG and CS tensor parameters are reported, the following general line shape fitting strategy is employed. First, a spectrum of a fast MAS sample is analyzed, yielding a CT centerband line shape which is reflective of only two parameters: C_Q and η_Q. The isotropic chemical shift is also obtained unambiguously. The spectrum of a stationary sample is then analyzed while keeping C_Q, η_Q, and δ_{iso} fixed at the values determined from the MAS sample. This leaves five adjustable parameters: the span, the skew, and α, β, and γ. Often there are approximately five key spectral features which must be properly fit and which therefore aid in converging on a unique spectral fit. However, whenever possible ^{37}Cl spectra are acquired in addition to ^{35}Cl spectra, which provides another unique piece of data to be fit (since the quadrupolar interactions for these nuclei differ but to a good approximation their CS tensors will be identical). Finally, spectra are acquired at more than one external applied magnetic field strength which again offers additional spectral data in which the relative effects of the quadrupolar and CS interactions differ due to their different field dependencies. Line shape fitting is performed interactively and does not rely on an automated fitting routine. In this way, emphasis is placed primarily on the frequencies of important spectral features, with a somewhat lesser emphasis on their relative intensities (since it is known that nonideal rf excitation may slightly affect the latter). Reported errors on the derived parameters are twice the value of the deviation from the best fit which is clearly detectable by visual inspection.

(iv) Quantum Chemical Calculations. Calculations of NMR interaction tensors were performed using Gaussian 03.[38] Models used in the calculations were built using atomic coordinates

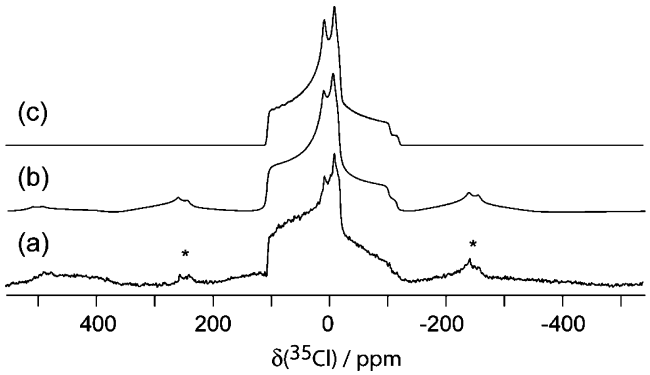

Figure 2. Solid-state ^{35}Cl MAS NMR spectroscopy of powdered L-tryptophan hydrochloride at 21.1 T. (a) Experimental spectrum obtained at a MAS rate of 22.000 kHz in a 3.2 mm MAS probe using a spin−echo sequence with high-power proton decoupling during acquisition. Spinning sidebands are denoted with asterisks. (b) Simulated spectrum which accounts for the finite spinning rate (generated using SIMPSON). (c) Simulated spectrum under the assumption of an infinite MAS rate (generated using WSOLIDS).

available from X-ray (L-arginine hydrochloride monohydrate,[39] L-tryptophan HCl,[40] L-lysine HCl[41]) or neutron (L-phenylalanine HCl,[42] glycine HCl,[43] L-valine HCl,[44] L-glutamic acid HCl,[45] L-tyrosine HCl[46]) diffraction studies. In some cases, proton coordinates were used as reported in the neutron diffraction studies; in other cases (and in the case of X-ray structures), the positions of the protons were optimized using quantum chemistry, while the positions of the heavy atoms (C, N, O, Cl) were held fixed. Geometry optimization convergence criteria were set at their default values. The restricted Hartree−Fock (RHF) method, or the B3LYP[47] or PBEPBE[48] functionals, were employed for geometry optimizations. Both Pople-type and Dunning-type basis sets were used. Some two-layer ONIOM calculations,[49−52] for which the high (inner) layer was treated at the MP2/6-31+G(d,p) level and the lower (outer) layer was treated at the AM1 level, were also carried out.

Subsequent to geometry optimization, EFG and nuclear magnetic shielding tensors were calculated using previously established optimum methods for amino acid hydrochlorides:[14] for the EFG tensor, the RHF method with the cc-pVTZ basis set on chlorine and the cc-pVDZ basis set on all other atoms; for the nuclear magnetic shielding tensor, the B3LYP method with the aug-cc-pVDZ basis set on chlorine and the cc-pVDZ basis set on all other atoms.

EFG and nuclear magnetic shielding output from Gaussian 03 was analyzed with an in-house program (EFGShield[53]) to extract the tensor magnitudes and orientations. Pyykkö's recommended value for $Q(^{35}\text{Cl})$, -8.165 fm^2, was used in eq 5.[54]

Results and Discussion

(i) Solid-State NMR Spectroscopy: L-Tryptophan Hydrochloride. Shown in Figure 2 is the ^{35}Cl MAS NMR spectrum of L-tryptophan hydrochloride obtained at 21.1 T with high-power proton decoupling during acquisition, along with the best-fit simulated spectra. The combination of the high magnetic field and a suitably fast MAS rate of 22 kHz enabled resolution of spinning sidebands from the central transition centerband. From the simulated spectra, the chlorine quadrupolar coupling constant, $C_Q(^{35}\text{Cl}) = \pm (5.05 \pm 0.04)$ MHz, asymmetry parameter (η_Q) of 0.86, and isotropic chemical shift (δ_{iso}) of 105 ppm are derived. Comparison of a simulated spectrum which incorporates the effects of a finite spinning speed (Figure 2b) and one which provides an ideal spectrum under the assumption of MAS at an

TABLE 1: Experimental Chlorine Quadrupolar and Chemical Shift Tensors for Selected Amino Acid Hydrochlorides

	$\lvert C_Q(^{35}Cl)\rvert$, MHz	η_Q	δ_{iso},[a] ppm	σ_{iso},[b] ppm	δ_{11}, ppm	δ_{22}, ppm	δ_{33}, ppm	Ω, ppm	κ	α, β, γ (deg)
L-tryptophan HCl[c]	5.05 ± 0.04	0.86 ± 0.03	105.0 ± 1.0	914.4	139.8	107.4	67.8	72 ± 5	0.10 ± 0.10	$90 \pm 15, 20 \pm 15, 2 \pm 20$
DL-arginine HCl monohydrate[d]	2.035 ± 0.020	0.98 ± 0.02	91.5 ± 1.0	927.9	117.7	96.7	60.2	57.5 ± 3.0	0.27 ± 0.10	$85 \pm 15, 77.5 \pm 12.0, 30 \pm 30$

[a] Chlorine-35 chemical shifts are with respect to the centerband ^{35}Cl resonance of solid powdered NaCl. [b] Converted from the chemical shift using the absolute shielding constant of 974 ppm for dilute aqueous NaCl[26] and the following relationship: δ(wrt infinitely dilute NaCl(aq)) = δ(wrt NaCl(s)) − 45.37 ppm.[56] [c] Quadrupolar parameters are based on fitting the ^{35}Cl MAS NMR spectrum shown in Figure 2. Chemical shift tensor parameters and Euler angles are based on interactive simultaneous fitting of a ^{35}Cl NMR spectrum of a stationary sample at 21.1 T, a ^{35}Cl NMR spectrum of a stationary sample at 11.75 T, and a ^{37}Cl NMR spectrum of a stationary sample at 21.1 T (all shown in Figure 3). [d] Quadrupolar parameters are based on fitting a ^{35}Cl MAS NMR spectrum at 11.75 T from reference 14, a ^{37}Cl MAS NMR spectrum at 11.75 T from reference 14, and a ^{35}Cl MAS NMR spectrum at 21.1 T (not shown). Chemical shift tensor parameters and Euler angles are based on interactive simultaneous fitting of a ^{35}Cl NMR spectrum of a stationary sample at 21.1 T and a ^{35}Cl NMR spectrum of a stationary sample at 11.75 T (see Figures 4 and 5).

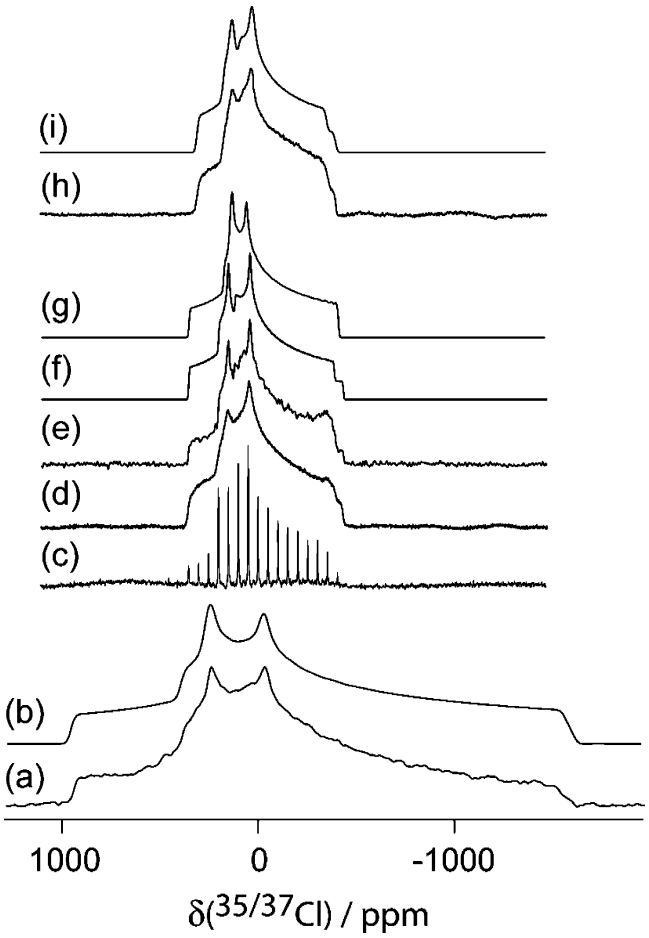

Figure 3. Solid-state chlorine NMR spectroscopy of powdered L-tryptophan hydrochloride under stationary conditions. (a) The experimental ^{35}Cl NMR spectrum obtained at 11.75 T using a hyperbolic secant spin−echo sequence with high-power proton decoupling during acquisition. (c) Experimental ^{35}Cl QCPMG NMR spectrum obtained at 21.1 T with proton decoupling, using a 3.2 mm MAS probe. (d) Experimental ^{35}Cl spin−echo NMR spectrum obtained at 21.1 T without proton decoupling, using a 5 mm solenoid probe. (e) Experimental ^{35}Cl NMR spectrum obtained at 21.1 T using a simple pulse-acquire sequence, with proton decoupling during acquisition, using a 3.2 mm MAS probe. (h) Experimental ^{37}Cl NMR spectrum obtained at 21.1 T using a single pulse (no ^{1}H decoupling), using a 5 mm solenoid probe. (b, f, and i) Simulated spectra for ^{35}Cl at 11.75 T, ^{35}Cl at 21.1 T, and ^{37}Cl at 21.1 T, respectively, which were generated using the parameters given in Table 1. (g) Simulation under the assumption of an isotropic CS tensor for ^{35}Cl at 21.1 T.

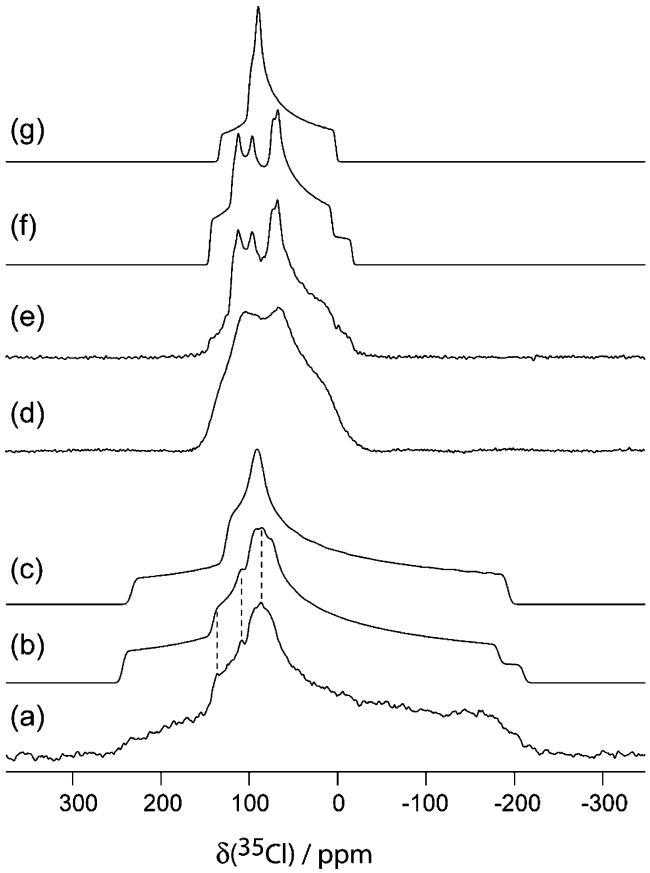

Figure 4. Solid-state chlorine-35 NMR spectroscopy of powdered DL-arginine hydrochloride monohydrate under stationary conditions. (a) The experimental ^{35}Cl NMR spectrum obtained at 11.75 T using a hyperbolic secant spin−echo sequence with high-power proton decoupling during acquisition. (d) Experimental ^{35}Cl spin−echo NMR spectrum obtained at 21.1 T without proton decoupling, using a 5 mm solenoid probe. (e) Experimental ^{35}Cl spin−echo NMR spectrum obtained at 21.1 T with proton decoupling, using a 3.2 mm MAS probe. (b and f) Simulated spectra for ^{35}Cl at 11.75 T and at 21.1 T, respectively, which were generated using the parameters given in Table 1. (c and g) Simulations under the assumption of an isotropic CS tensor for ^{35}Cl at 11.75 T and at 21.1 T, respectively.

infinite rate (Figure 2c) indicates very minor differences, indicating that the MAS rate used experimentally is sufficiently large to enable reliable spectral interpretation. Such interpretation would be more difficult in lower magnetic fields and/or with slower MAS rates, where sidebands may overlap with the centerband. The value of $|C_Q|$ obtained for L-Trp HCl lies between those reported previously for L-isoleucine HCl (4.39 ± 0.05 MHz) and L-valine HCl (5.89 ± 0.05 MHz).[14] Thus, the relatively large value of $C_Q(^{35}Cl)$ obtained for L-Trp HCl is consistent with the previous finding that HCl salts of hydrophobic amino acids exhibit relatively large chlorine quadrupolar coupling constants.[14]

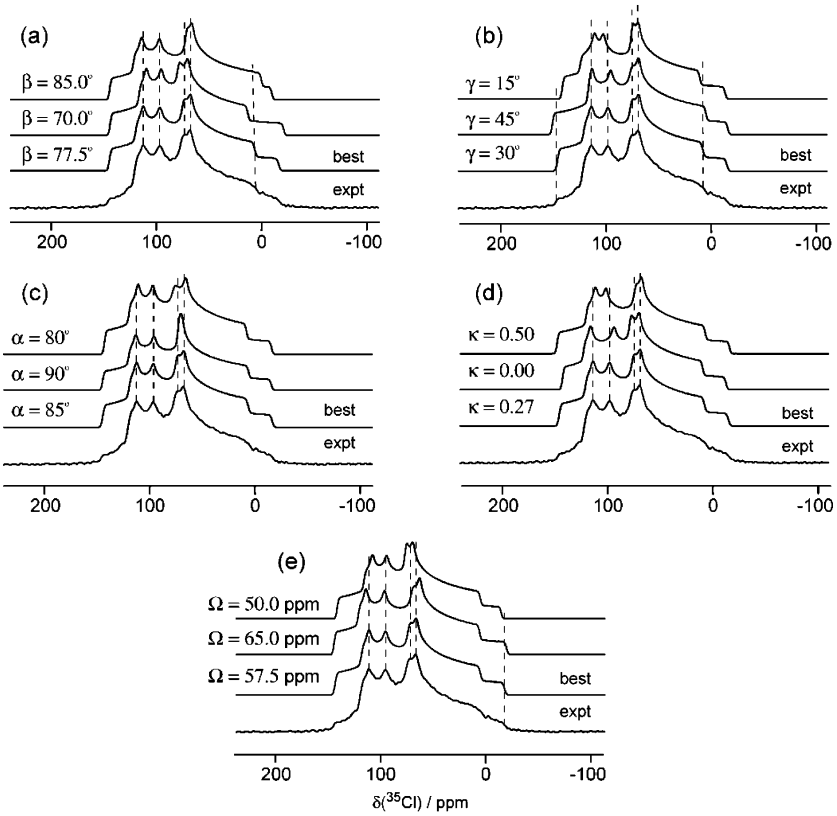

Figure 5. Sensitivity of the ^{35}Cl NMR spectrum of stationary solid powdered DL-arginine hydrochloride monohydrate to the magnitude of the chlorine chemical shift tensor and its orientation relative to the chlorine EFG tensor. In each part, the experimental spin−echo spectrum obtained at 21.1 T is shown in the lower trace and the best-fit simulated spectrum is shown directly above. The parameters β, γ, α, κ, and Ω are varied in parts a, b, c, d, and e, respectively. Dashed lines emphasize spectral features which are particularly sensitive to the parameter being varied.

Having established the quadrupolar parameters, chlorine NMR spectra of stationary powdered samples of L-Trp HCl were acquired and analyzed to provide information on the CS tensor and the orientation of its PAS relative to that of the EFG tensor. Presented in Figure 3 are chlorine-35/37 NMR spectra of L-Trp HCl acquired under stationary conditions. Shown in part (a) is the ^{35}Cl NMR spectrum acquired at 11.75 T using the hyperbolic secant spin−echo sequence. It was not possible to definitively determine the chlorine CS tensor magnitude and orientation from this spectrum. Chlorine-35 and chlorine-37 NMR spectra were therefore acquired at 21.1 T and are presented in Figure 3d and 3h, respectively. A ^{35}Cl QCPMG NMR spectrum was also acquired (Figure 3c), which reflects the envelope of the powder pattern. For most hydrochloride salts we have examined, ^{35}Cl QCPMG spikelets may be easily seen after one complete phase cycle.

To conclusively and precisely determine the EFG and CS tensor magnitudes, and their relative orientations, high-power proton decoupling was extremely beneficial in the case of L-Trp HCl (Figure 3e) and essential in other cases (*vide infra*). The span of the chlorine CS tensor, $\Omega = 72 \pm 5$ ppm, is intermediate compared to other amino acid hydrochlorides. For example, $\Omega = 26 \pm 10$ ppm in L-lysine HCl and $\Omega = 129 \pm 20$ ppm in L-phenylalanine HCl.[14]

Although precise temperature measurements on the sample were not performed during the experiments, it is apparent that the spectrum corresponding to the sample undergoing fast MAS is better fit with a slightly smaller (∼0.02 MHz) value of C_Q(^{35}Cl) than is the spectrum of the stationary sample (Figure 3). The errors in the quadrupolar parameters reported in Table 1 for L-Trp HCl are therefore likely dominated by temperature effects; however, we note that the error in C_Q is still on the order of only 1% of its magnitude. This effect appears to be smaller than that observed by Honda for solid *n*-alkylammonium chlorides at room temperature.[55] The temperature dependence of the chlorine NMR interaction tensors in hydrochloride salts of amino acids will be investigated in more detail in due course.

(ii) Importance of Proton Decoupling. As alluded to above, high-power proton decoupling was found to be critical in resolving key spectral features in the $^{35/37}$Cl NMR spectra of some solid amino acid hydrochlorides. Typical hydrogen-bonded proton-chlorine distances in amino acid hydrochlorides for which neutron diffraction structures are available range from 1.990 Å (for an OH···Cl contact in L-valine HCl[44]) to 2.593 Å (for an NH···Cl contact in glycine HCl[43]). The magnitude of the ^{1}H-^{35}Cl direct dipolar coupling constant,

$$R_{DD} = \frac{\mu_0}{4\pi}\frac{\hbar}{2\pi}\gamma_{^1H}\gamma_{^{35}Cl}\langle r_{H-Cl}^{-3}\rangle,$$

therefore ranges from 676 to 1495 Hz under the assumption of negligible motion. When a chloride ion is surrounded by several protons in close contact, as is the case for the amino acid hydrochlorides, the cumulative broadening effect on the chlorine solid-state NMR spectrum may become severe enough to completely obscure key spectral features. This is illustrated most strikingly in the case of DL-arginine hydrochloride monohydrate (Figure 4). Shown in Figure 4d is the ^{35}Cl NMR spectrum of a stationary powdered sample of DL-Arg HCl•H_2O acquired at 21.1 T without proton decoupling, and Figure 4e depicts the same spectrum acquired with high-power proton decoupling. Because the value of $|C_Q|$ is small (2.035 ± 0.020 MHz, see Table 1), even a moderate degree of anisotropy in the chlorine CS tensor ($\Omega = 57.5$ ppm in this case) has a drastic impact on the spectral

line shape at 21.1 T. Almost all of the important spectral features are missing in the absence of proton decoupling. In fact, this prevented us from precisely determining the span of the chlorine CS tensor in DL-Arg HCl·H_2O in a previous report.[14] The simulated spectrum, incorporating the effects of anisotropic magnetic shielding and the quadrupolar interaction, presented in Figure 4f, very successfully reproduces the experimental spectrum (Figure 4e). It is clear that the CS tensor parameters could not have been determined on the basis of the proton-coupled spectrum shown in Figure 4d. Furthermore, the proton-decoupled spectrum is impossible to properly simulate if the CS tensor anisotropy is ignored; the simulated spectrum of a stationary sample based solely on the quadrupolar interaction is presented in Figure 4g and none of the important spectral discontinuities are reproduced. In fact, attempts at estimating, e.g., η_Q, from visual inspection of the proton-coupled spectrum in Figure 4d would be erroneous.

The ^{35}Cl NMR spectrum of DL-Arg HCl·H_2O acquired under stationary conditions at 11.75 T (Figure 4a) was not possible to simulate in the absence of the data acquired at 21.1 T. In particular, there are three key spectral features (indicated in Figure 4) which are very sensitive to the precise magnitude and orientation of the CS tensor with respect to the EFG tensor. The extreme sensitivity of the ^{35}Cl NMR spectrum of a stationary sample of DL-Arg HCl·H_2O acquired at 21.1 T to the magnitude and orientation of the chlorine CS tensor relative to the EFG tensor is demonstrated in Figure 5. There are approximately seven key spectral features which must be reproduced, and the simulated spectrum is markedly sensitive to variations in Ω, κ, and the three Euler angles α, β, and γ. The experimental spectrum is a useful example of how the effects of an anisotropic chemical shift and a moderate quadrupolar interaction conspire to produce particularly detailed and informative line shapes in high magnetic fields.

Another example of the importance of high-power proton decoupling in the analysis of chlorine NMR spectra of solid amino acid hydrochlorides exhibiting relatively small values of $C_Q(^{35}Cl)$ is presented in Figure 6. Our previous work successfully characterized the magnitude and orientation of the chlorine CS tensor in L-lysine HCl on the basis of data obtained at 11.75 T.[14] The ^{35}Cl NMR spectrum obtained at 21.1 T without proton decoupling (Figure 6a) was not useful in the refinement of these parameters. Proton decoupling (Figure 6b) greatly improves the spectrum and a successful simulation (Figure 6c) is achieved using the same parameters as used to simulate the previously obtained spectra at 11.75 T. The simulated spectrum shown in Figure 6d serves again to emphasize the poor fit with experiment when the effects of anisotropic magnetic shielding are ignored. Excellent agreement with the previously reported quadrupolar parameters ($|C_Q(^{35}Cl)| = 2.49 \pm 0.01$ MHz; $\eta_Q = 0.42 \pm 0.02$)[14] was obtained from a ^{35}Cl MAS NMR spectrum of L-lysine HCl obtained at 21.1 T (Figure 6(e),(f)).

A notable improvement in the ^{35}Cl NMR spectrum of a stationary spectrum of L-glutamic acid HCl at 21.1 T was also achieved with the addition of proton decoupling (Figure 7a,b). There are several important spectral features which become superbly resolved. The spectrum was successfully simulated using the available quadrupolar and CS tensor parameters;[14] however, the present results provide extra confidence in the conclusions reached without ^{1}H decoupling.

It is important to point out that as the chlorine quadrupolar interaction becomes larger, the effect of spectral line broadening due to ^{35}Cl−^{1}H dipolar interactions becomes less important. For example, chloride sites with $C_Q(^{35}Cl)$ in excess of ~5 MHz give excellent spectra at 21.1 T without proton decoupling. In general, it is always important to record chlorine NMR spectra with at least two different magnetic field strengths, when possible, for reliable spectral interpretation.

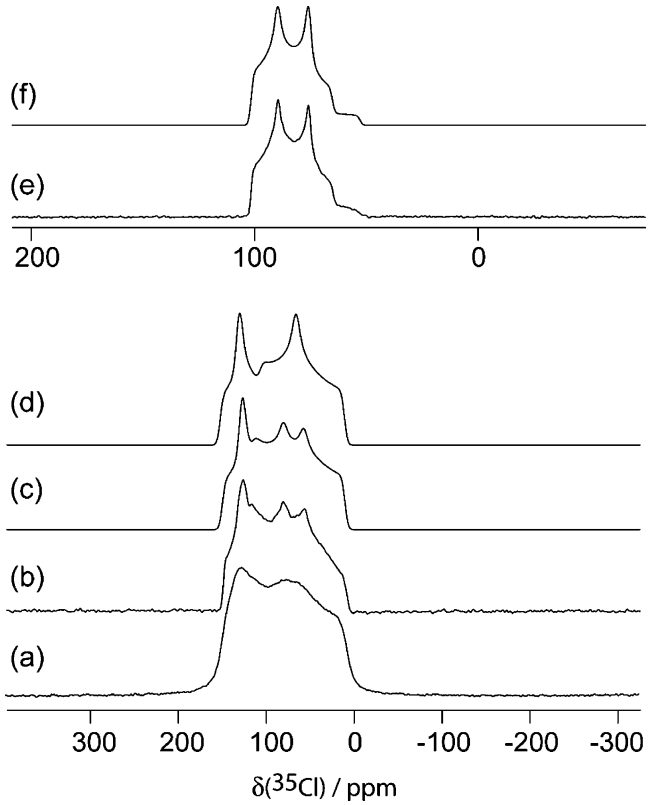

Figure 6. Solid-state ^{35}Cl NMR spectroscopy of powdered L-lysine hydrochloride at 21.1 T. (a) The experimental ^{35}Cl NMR spectrum obtained for a stationary sample at 21.1 T without proton decoupling, using a 5 mm solenoid probe. (b) Experimental ^{35}Cl spin−echo NMR spectrum obtained for a stationary sample at 21.1 T with proton decoupling, using a 3.2 mm MAS probe. (c) Corresponding simulated spectrum; the parameters used are consistent with those reported in reference 14. (d) The same spectral simulation, except with the span of the CS tensor set to zero. (e) Experimental ^{35}Cl spin−echo MAS NMR spectrum (MAS rate = 17.000 kHz) obtained at 21.1 T with proton decoupling, using a 3.2 mm MAS probe. (f) The corresponding spectral simulation, using the parameters given in reference 14.

One of the interesting conclusions which may be drawn from the new data obtained for L-Trp HCl and DL-Arg HCl·H_2O, combined with existing CS tensor data for other amino acid hydrochlorides,[14,56] is that the span of the chlorine CS tensor seems to be smaller for salts of hydrophilic amino acids than for salts of hydrophobic amino acids (see Figure 8). This trend is similar to the trend observed previously for the chlorine quadrupolar coupling constants; however, it is clear that the EFG and CS tensors report on different aspects of the local molecular geometry and electronic structure. This is confirmed by the poor correlation between C_Q and Ω (Supporting Information).

(iii) Refinement of Hydrogen-Bonded Proton Positions. It was previously shown[14] for amino acid hydrochlorides that, as long as a high-quality neutron diffraction structure which provides reliable proton positions is available, essentially quantitative agreement with experimental values of $C_Q(^{35}Cl)$ and Ω is achievable using quantum chemical calculations. In this section, we explore the possibility of using chlorine quadrupolar and CS tensor data as a cross-validation of quantum-chemically refined proton positions for X-ray structures, wherein proton positions are generally not determined. Therefore, the primary purpose of the quantum chemical calculations is to provide

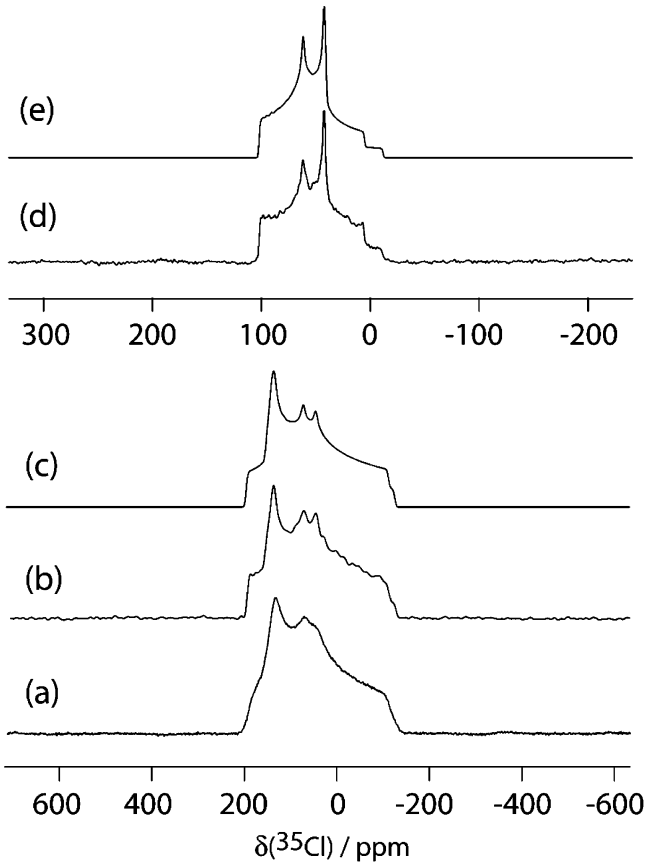

Figure 7. Solid-state ^{35}Cl NMR spectroscopy of powdered L-glutamic acid hydrochloride at 21.1 T. (a) The experimental ^{35}Cl NMR spectrum obtained for a stationary sample at 21.1 T without proton decoupling, using a 5 mm solenoid probe (same as shown in Figure 9d of reference 14; shown here for comparison with part b). (b) Experimental ^{35}Cl spin−echo NMR spectrum obtained for a stationary sample at 21.1 T with proton decoupling, using a 3.2 mm MAS probe. (c) Corresponding simulated spectrum using the parameters reported in ref 14. (d) Experimental ^{35}Cl MAS NMR spectrum (MAS rate = 17.000 kHz) obtained at 21.1 T with proton decoupling, using a 3.2 mm MAS probe. (e) The corresponding spectral simulation, using the quadrupolar parameters reported in reference 14.

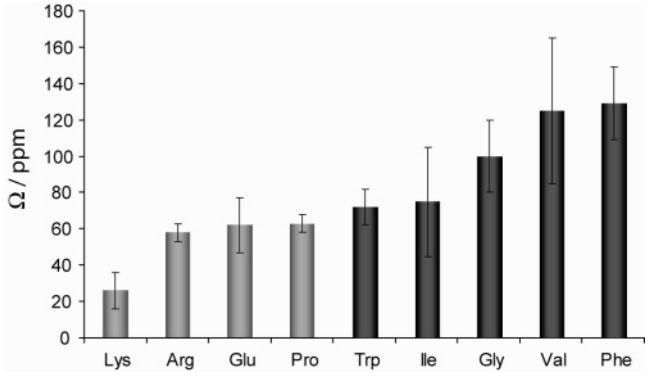

Figure 8. Experimental chlorine chemical shift tensor spans for hydrophilic (light gray, left) and hydrophobic (dark gray, right) amino acid hydrochlorides. Data are from Table 1 and reference 14.

optimized proton positions. The accuracy of these positions will be assessed through a second series of calculations which will provide quadrupolar and CS tensor data for use in the cross-validation by experimental data.

The first step undertaken was to start with atomic coordinates from neutron diffraction structures (L-phenylalanine HCl and glycine HCl) and allow the proton positions to be optimized

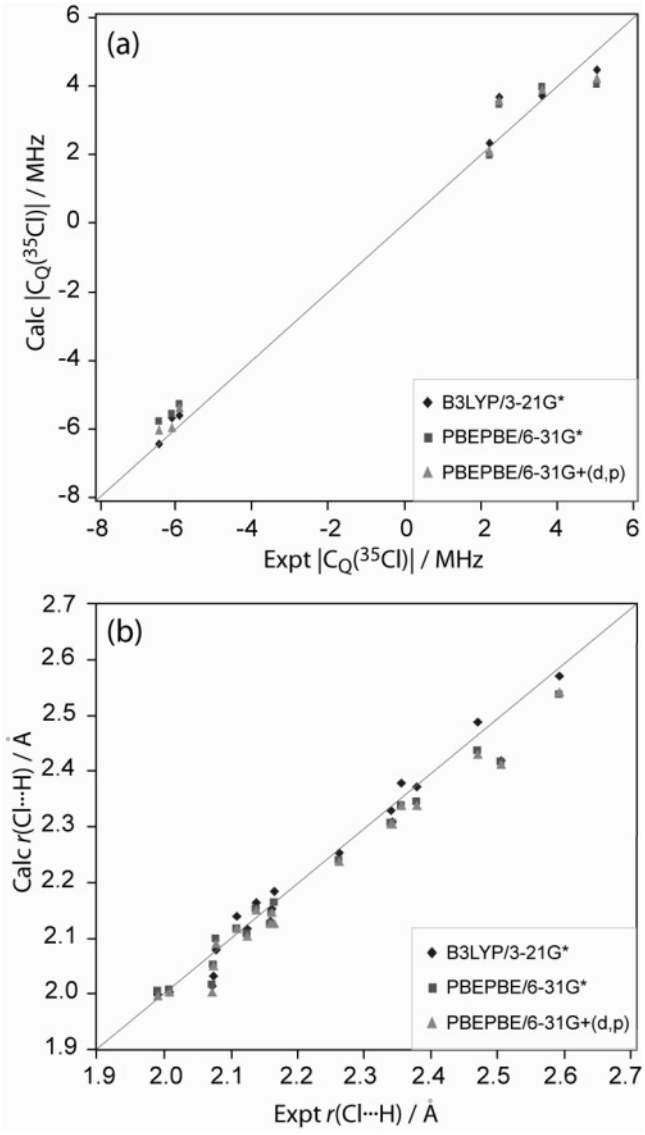

Figure 9. (a) Plot of calculated vs experimental chlorine-35 nuclear quadrupolar coupling constants for Gly HCl, L-Tyr HCl, L-Lys HCl, L-Trp HCl, L-Phe HCl, L-Glu HCl, L-Val HCl. As described in the text, proton positions have been optimized at either the B3LYP/3-21G* (diamonds), PBEPBE/6-31G* (squares), or PBEPBE/6-31G+(d,p) (triangles) level prior to EFG tensor calculations at the RHF/cc-pVTZ/cc-pVDZ level. Linear regression and root-mean-square deviation (rmsd) results: C_Q(calc) = 0.9867C_Q(expt) + 0.2041 MHz, R = 0.9947, rmsd = 0.54 MHz (B3LYP/3-21G*); C_Q(calc) = 0.9284C_Q(expt) + 0.2053 MHz, R = 0.9930, rmsd = 0.68 MHz (PBEPBE/6-31G*); C_Q(calc) = 0.9619C_Q(expt) + 0.1659 MHz, R = 0.9937, rmsd = 0.58 MHz (PBEPBE/6-31+G(d,p)). (b) Plot of calculated vs experimental chlorine-hydrogen distances for hydrogens involved in hydrogen bonding (i.e., OH or NH type hydrogens) with the chloride ion for L-Glu HCl, Gly HCl, L-Val HCl, L-Phe HCl, L-Tyr HCl. Experimental distances are from neutron diffraction structures (see text). Calculated distances result from partial geometry optimizations (see text) at the B3LYP/3-21G* (diamonds), PBEPBE/6-31G* (squares), or PBEPBE/6-31G+(d,p) (triangles) level. Linear regression and root-mean-square deviation (rmsd) results: r(calc) = 0.962r(expt) + 0.0746 Å, R = 0.9852, rmsd = 0.031 Å (B3LYP/3-21G*); r(calc) = 0.8903r(expt) + 0.2229 Å, R = 0.9918, rmsd = 0.035 Å (PBEPBE/6-31G*); r(calc) = 0.9016r(expt) + 0.1928 Å, R = 0.9910, rmsd = 0.038 Å (PBEPBE/6-31+G(d,p)).

quantum chemically. The previously established[14] RHF/cc-pVTZ/cc-pVDZ (cc-pVTZ on Cl and cc-pVDZ on all other atoms) method was then used to calculate C_Q and, in a third calculation, the B3LYP/aug-cc-pVDZ/cc-pVDZ (aug-cc-pVDZ

TABLE 2: Quantum Chemical Calculations of Chlorine Nuclear Quadrupolar Coupling Constants and Chemical Shift Tensor Spans for L-Phenylalanine Hydrochloride[a]

optimization method[b]	C_Q(^{35}Cl), MHz (RHF/cc-pVTZ/cc-pVDZ)	Ω, ppm (B3LYP/aug-cc-pVDZ/cc-pVDZ)
RHF/3-21G*	−5.07	110
RHF/6-31G*	−5.00	110
RHF/cc-pVDZ	−4.94	111
B3LYP/3-21G*	−5.69	110
B3LYP/6-31G*	−5.39	112
B3LYP/6-31+G(d,p)	−5.54	117
B3LYP/cc-pVDZ	−5.44	113
PBEPBE/3-21G*	−6.15	111
PBEPBE/6-31G*	−5.57	112
PBEPBE/6-31+G(d,p)	−5.96	118
PBEPBE/cc-pVDZ	−5.69	114
ONIOM (MP2/6-31+G(d,p): AM1)	−5.20	115
expt[14]	−6.08 ± 0.05	129 ± 20

[a] All calculations of C_Q were carried out at the RHF level with the cc-pVTZ basis set on chlorine and the cc-pVDZ basis set on all other atoms, after geometry optimization at the level indicated. All calculations of Ω were carried out at the B3LYP level with the aug-cc-pVDZ basis set on chlorine and the cc-pVDZ basis set on all other atoms, after geometry optimization at the level indicated. [b] In all cases, a quantum chemical optimization of the geometry of the hydrogen atoms hydrogen bonded to the chloride ion (and all other hydrogens in the model) was performed while the heavy atoms (C, N, O, Cl) were held fixed at the positions available from the experimental neutron diffraction structure.

TABLE 3: Quantum Chemical Calculations of Chlorine Nuclear Quadrupolar Coupling Constants and Chemical Shift Tensor Spans for Glycine Hydrochloride[a]

optimization method[b]	C_Q(^{35}Cl), MHz (RHF/cc-pVTZ/cc-pVDZ)	Ω, ppm (B3LYP/aug-cc-pVDZ/cc-pVDZ)
RHF/3-21G*	−5.19	94.9
RHF/6-31G*	−4.49	92.0
RHF/cc-pVDZ	−4.56	92.4
RHF/aug-cc-pVDZ	−4.76	92.4
B3LYP/3-21G*	−6.42	104.7
B3LYP/6-31G*	−5.51	100.0
B3LYP/6-31+G(d,p)	−5.58	101.1
B3LYP/cc-pVDZ	−5.55	100.3
B3LYP/aug-cc-pVDZ	−5.73	101.7
PBEPBE/3-21G*	−6.97	110.8
PBEPBE/6-31G*	−5.80	103.0
PBEPBE/6-31+G(d,p)	−6.03	103.8
PBEPBE/cc-pVDZ	−5.98	104.4
PBEPBE/aug-cc-pVDZ	−6.19	104.8
expt[14]	−6.42 ± 0.05	100 ± 20

[a] All calculations of C_Q were carried out at the RHF level with the cc-pVTZ basis set on chlorine and the cc-pVDZ basis set on all other atoms, after geometry optimization at the level indicated. All calculations of Ω were carried out at the B3LYP level with the aug-cc-pVDZ basis set on chlorine and the cc-pVDZ basis set on all other atoms, after geometry optimization at the level indicated. [b] In all cases, quantum chemical optimization of the geometry of the hydrogen atoms hydrogen bonded to the chloride ion (and all other hydrogens in the model) was performed while the heavy atoms (C, N, O, Cl) were held fixed at the positions available from the experimental neutron diffraction structure.

on Cl and cc-pVDZ on all other atoms) method was used to calculate the chlorine magnetic shielding tensor to obtain Ω. Since the proton positions are known with high precision to begin with in the neutron diffraction structures, this strategy allowed us to confirm that the geometry optimizations provided realistic and reliable proton positions in addition to simply providing structures which resulted in chlorine NMR interaction tensors in good agreement with experimental values. The results of this procedure are summarized in Table 2 (L-Phe HCl) and Table 3 (Gly HCl) (see also Supporting Information). All calculated results are in reasonable agreement with experiment; however, quantitative agreement is lacking in many cases particularly in the case of C_Q. The span does not appear to be very sensitive to the method of optimization employed, particularly when compared to the sensitivity of C_Q. From these results, we conclude that the B3LYP/3-21G*, PBEPBE/6-31G*, and PBEPBE/6-31+G(d,p) methods provide structures with reliable proton positions and which can be subsequently used for calculations of the chlorine EFG and magnetic shielding tensors. Many different optimization calculations were attempted, including RHF calculations and an ONIOM (MP2: AM1) calculation, and calculations with much larger basis sets (Tables 2 and 3).

The B3LYP/3-21G*, PBEPBE/6-31G*, and PBEPBE/6-31+G(d,p) methods were next applied to the remaining three amino acid hydrochlorides for which neutron diffraction structures are available (L-Val HCl, L-Glu HCl, L-Tyr HCl). The results are summarized in the Supporting Information. A plot of calculated vs experimental values of C_Q(^{35}Cl) (Figure 9a) as well as a plot of the calculated vs experimental hydrogen-bond Cl···H distances (Figure 9b) indicates that the relatively low level B3LYP/3-21G* optimization method performs best. Quadrupolar coupling constants are predicted (in a subsequent calculation at the RHF/cc-pVTZ/cc-pVDZ level) with a root-mean-square deviation (rmsd) of 0.54 MHz and Cl···H distances with an rmsd of 0.031 Å.

The proton positions around chloride in L-Trp HCl and L-Lys HCl were next determined using the experimental values of Ω and C_Q(^{35}Cl) as a cross-validation of the geometry optimization (Table 4). The resulting calculated values of Ω and C_Q(^{35}Cl) were compared to the available experimental results (see Table 4). Importantly, since neutron diffraction structures are not

TABLE 4: Dependence of Quantum Chemically-Calculated Chlorine Nuclear Quadrupolar Coupling Constants and Chemical Shift Tensor Spans on Initial Proton Geometry Optimization Method[a]

	optimization method[b]	$\|C_Q(^{35}Cl)\|$, MHz (RHF/cc-pVTZ/cc-pVDZ)	Ω, ppm (B3LYP/aug-cc-pVDZ/cc-pVDZ)	d_1,[c] Å	d_2, Å	d_3, Å	d_4, Å
L-tryptophan HCl	B3LYP/3-21G*	4.49	76.9	2.05	2.17	2.18	2.33
	PBEPBE/6-31G*	4.02	69.5	2.06	2.11	2.17	2.29
	PBEPBE/6-31+G(d,p)	4.22	69.2	2.06	2.12	2.16	2.28
	expt	5.05 ± 0.04	72 ± 5	n/a	n/a	n/a	n/a
L-lysine HCl	B3LYP/3-21G*	3.69	28.5	2.16	2.44	2.16	2.42
	PBEPBE/6-31G*	3.47	27.4	2.15	2.49	2.16	2.42
	PBEPBE/6-31+G(d,p)	3.57	28.4	2.16	2.44	2.16	2.42
	expt[14]	2.49 ± 0.01	26 ± 10	n/a	n/a	n/a	n/a

[a] All calculations of C_Q were carried out at the RHF level with the cc-pVTZ basis set on chlorine and the cc-pVDZ basis set on all other atoms, after geometry optimization at the level indicated. All calculations of Ω were carried out at the B3LYP level with the aug-cc-pVDZ basis set on chlorine and the cc-pVDZ basis set on all other atoms, after geometry optimization at the level indicated. [b] Quantum chemical optimization of the geometry of the hydrogen atoms hydrogen bonded to the chloride ion (and all other hydrogens in the model) was performed while the heavy atoms (C, N, O, Cl) were held fixed at the positions available from the experimental X-ray diffraction structure. [c] d_1, d_2, d_3, d_4 refer to the four nearest-neighbor hydrogen-chlorine distances. See Supporting Information.

available for these amino acid hydrochlorides, geometry optimization of the proton positions *must* be employed in order to attempt quantum chemical calculations of the EFG and nuclear magnetic shielding tensors.

The results in Tables 2−4 (and Supporting Information) indicate that for hydrochloride salts of amino acids, the chloride quadrupolar coupling constant may easily be predicted within 1 MHz when a neutron diffraction structure is unavailable. L-lysine HCl represents by far the worst case in terms of percentage difference between the experimental and calculated values of $|C_Q(^{35}Cl)|$. For example, using the B3LYP/3-21G* optimization method for protons, this difference is 12, 7, 0, −4, 5, and 3%, respectively, for L-Trp HCl, L-Phe HCl, Gly HCl, L-Tyr HCl, L-Val HCl, and L-Glu HCl. In cases where chloride ions are not effectively isolated from other chloride ions (e.g., L-Pro HCl[57]), it is likely that the current methods will fail since there will be significant longer-range contributions to the EFG tensor at a given chloride site.

A final interesting case is that of DL-Arg HCl•H_2O. This material is unique in the present study in that it contains water molecules in close contact with Cl^- in addition to hydrogen bonds to the arginine sidechains. The RHF/cc-pVTZ/cc-pVDZ calculated value of $|C_Q(^{35}Cl)|$ (after B3LYP/3-21G* optimization of proton positions), 4.84 MHz, is significantly larger than the precise experimental value of 2.035 ± 0.020 MHz. Given the unique presence of the water molecules around chloride, this result suggests that notable motion of the water molecules in the crystal could be leading to a reduction in the apparent EFG at chloride. Further experiments will need to be performed to confirm this possibility.

Conclusions

Solid-state chlorine NMR data for L-tryptophan hydrochloride and DL-arginine hydrochloride monohydrate have helped in the elucidation of a trend in the spans of the chlorine chemical shift tensors in amino acid hydrochlorides. Larger spans are observed for hydrochloride salts of hydrophobic amino acids and smaller spans are observed for hydrochloride salts of hydrophilic amino acids. While this trend parallels the previously reported correlation[14] between the chlorine quadrupolar coupling constant and the nature of the amino acid side chain in hydrophilic and hydrophobic amino acids, there is no strong correlation between Ω and C_Q themselves, thereby intimating that Ω provides unique information on the chloride ion binding environment. A magnetic field strength of 21.1 T and high-power proton decoupling were crucial factors in proper spectral interpretation. In particular, high-power proton decoupling is critical when examining systems which exhibit small ^{35}Cl quadrupolar coupling constants (i.e., less than ~3 MHz) because in high magnetic fields the second-order quadrupolar broadening of the central transition is reduced while the $^{35/37}Cl-^{1}H$ dipolar broadening is constant.

Quantum-chemically optimized hydrogen-bonded proton positions in a series of amino acid hydrochlorides were cross-validated against experimental chlorine EFG and chemical shift tensors. From these extensive calculations, we conclude that, in cases where heavy-atom positions are known but proton positions are lacking (e.g., due to the availability of an X-ray diffraction structure and unavailability of a neutron diffraction structure), the B3LYP/3-21G* method is suitable for optimization of the proton positions. Chlorine-35 quadrupolar coupling constants are subsequently generally predicted, using quantum chemistry, to within 15% of the experimental solid-state values. Calculated chlorine chemical shift tensor spans are found to be significantly less sensitive to the positions of the protons than are the quadrupolar coupling constants. The combined experimental−theoretical method represents a step toward incorporating experimental chlorine NMR interaction tensors as valuable structural restraints in the description of chloride ion binding sites in amino acid hydrochlorides and larger, structurally similar systems.

Acknowledgment. Glenn Facey and Victor Terskikh are thanked for their technical assistance and for many helpful comments. We thank Rod Wasylishen, Renée Siegel, and Tom Nakashima for providing the pulse code for the hyperbolic secant echo sequence. Jamie Bennett (NRC, Ottawa) is thanked for construction of the 5 mm NMR probe used at 21.1 T. We thank Claudio Carra for helpful discussions. Access to the 900 MHz NMR spectrometer was provided by the National Ultrahigh Field NMR Facility for Solids (Ottawa, Canada), a national research facility funded by the Canada Foundation for Innovation, the Ontario Innovation Trust, Recherche Québec, the National Research Council of Canada, and Bruker BioSpin and managed by the University of Ottawa (www.nmr900.ca). The Natural Sciences and Engineering Research Council of Canada (NSERC) is acknowledged for a Major Resources Support grant. Some quantum chemical calculations were carried out using the High Performance Virtual Computing Laboratory (HPCVL). D.L.B. thanks NSERC and the University of Ottawa Faculty of Science for generous funding.

Supporting Information Available: Tables containing hydrogen bond distances, calculated values of η_Q, and principal

components of the magnetic shielding tensor for all methods; correlation plot for C_Q and Ω; atomic coordinates for selected structures of amino acid hydrochlorides with optimized proton positions; figures showing structural models used for EFG and magnetic shielding tensor calculations. This material is available free of charge via the Internet at http://pubs.acs.org.

References and Notes

(1) Stebbins, J. F.; Du, L.-S.; Kroeker, S.; Neuhoff, P.; Rice, D.; Frye, J.; Jakobsen, H. J. *Solid State Nucl. Magn. Reson.* **2002**, *21*, 105.

(2) Sandland, T. O.; Du, L. S.; Stebbins, J. F.; Webster, J. D. *Geochim. Cosmochim. Acta* **2004**, *68*, 5059.

(3) Stebbins, J. F.; Du, L. S. *Am. Mineral.* **2002**, *87*, 359.

(4) Gan, Z.; Gor'kov, P.; Cross, T. A.; Samoson, A.; Massiot, D. *J. Am. Chem. Soc.* **2002**, *124*, 5634.

(5) Lipton, A. S.; Heck, R. W.; Ellis, P. D. *J. Am. Chem. Soc.* **2004**, *126*, 4735.

(6) Lipton, A. S.; Bergquist, C.; Parkin, G.; Ellis, P. D. *J. Am. Chem. Soc.* **2003**, *125*, 3768.

(7) Lipton, A. S.; Wright, T. A.; Bowman, M. K.; Reger, D. L.; Ellis, P. D. *J. Am. Chem. Soc.* **2002**, *124*, 5850.

(8) Lipton, A. S.; Buchko, G. W.; Sears, J. A.; Kennedy, M. A.; Ellis, P. D. *J. Am. Chem. Soc.* **2001**, *123*, 992.

(9) Wu, G.; Wong, A.; Gan, Z.; Davis, J. T. *J. Am. Chem. Soc.* **2003**, *125*, 7182.

(10) Wong, A.; Whitehead, R. D.; Gan, Z.; Wu, G. *J. Phys. Chem. A* **2004**, *108*, 10551.

(11) Hu, J.; Chekmenev, E. Y.; Gan, Z.; Gor'kov, P. L.; Saha, S.; Brey, W. W.; Cross, T. A. *J. Am. Chem. Soc.* **2005**, *127*, 11922.

(12) Fu, R.; Brey, W. W.; Shetty, K.; Gor'kov, P.; Saha, S.; Long, J. R.; Grant, S. C.; Chekmenev, E. Y.; Hu, J.; Gan, Z.; Sharma, M.; Zhang, F.; Logan, T. M.; Brüschweller, R.; Edison, A.; Blue, A.; Dixon, I. R.; Markiewicz, W. D.; Cross, T. A. *J. Magn. Reson.* **2005**, *177*, 1.

(13) Bryce, D. L.; Sward, G. D. *Magn. Reson. Chem.* **2006**, *44*, 409.

(14) Bryce, D. L.; Sward, G. D.; Adiga, S. *J. Am. Chem. Soc.* **2006**, *128*, 2121.

(15) Gervais, C.; Dupree, R.; Pike, K. J.; Bonhomme, C.; Profeta, M.; Pickard, C. J.; Mauri, F. *J. Phys. Chem. A* **2005**, *109*, 6960.

(16) Dong, C.; Flecks, S.; Unversucht, S.; Haupt, C.; van Pée, K.-H.; Naismith, J. H. *Science* **2005**, *309*, 2216.

(17) Guggino, W. B., Ed. *Chloride Channels: Current Topics in Membranes, volume 42*, Kleinzeller, A.; Fambrough, D. M., Eds., Academic Press: San Diego, 1994.

(18) Ashcroft, F. M. *Ion Channels and Disease*; Academic Press: San Diego, 2000.

(19) Loewen, M. E.; Forsyth, G. W. *Physiol. Rev.* **2005**, *85*, 1061.

(20) Dutzler, R.; Campbell, E. B.; Cadene, M.; Chait, B. T.; MacKinnon, R. *Nature* **2002**, *415*, 287.

(21) Ashbrook, S. E.; Duer, M. J. *Concepts Magn. Reson.* **2006**, *28A*, 183.

(22) Power, W. P.; Wasylishen, R. E.; Mooibroek, S.; Pettitt, B. A.; Danchura, W. *J. Phys. Chem.* **1990**, *94*, 591.

(23) Chu, P. J.; Gerstein, B. C. *J. Chem. Phys.* **1989**, *91*, 2081.

(24) Wi, S.; Ashbrook, S. E.; Wimperis, S.; Frydman, L. *J. Chem. Phys.* **2003**, *118*, 3131.

(25) Mason, J. *Solid State Nucl. Magn. Reson.* **1993**, *2*, 285.

(26) Gee, M.; Wasylishen, R. E.; Laaksonen, A. *J. Phys. Chem. A* **1999**, *103*, 10805.

(27) Siegel, R.; Nakashima, T. T.; Wasylishen, R. E. *Chem. Phys. Lett.* **2004**, *388*, 441.

(28) Siegel, R.; Nakashima, T. T.; Wasylishen, R. E. *Concepts Magn. Reson. Part A* **2005**, *26A*, 47.

(29) Carr, H. Y.; Purcell, E. M. *Phys. Rev.* **1954**, *94*, 630.

(30) Meiboom, S.; Gill, D. *Rev. Sci. Instrum.* **1958**, *29*, 688.

(31) Cheng, J. T.; Ellis, P. D. *J. Phys. Chem.* **1989**, *93*, 2549.

(32) Larsen, F. H.; Jakobsen, H. J.; Ellis, P. D.; Nielsen, N. Chr. *J. Phys. Chem. A* **1997**, *101*, 8597.

(33) Eichele, K.; Wasylishen R. E. WSOLIDS NMR Simulation Package, version 1.17.30; Dalhousie University, Halifax, 2001.

(34) Alderman, D. W.; Solum, M. S.; Grant, D. M. *J. Chem. Phys.* **1986**, *84*, 3717.

(35) Bak, M.; Rasmussen, J. T.; Nielsen, N. C. *J. Magn. Reson.* **2000**, *147*, 296.

(36) Downloaded from http://nmr.imsb.au.dk/download/simpson/.

(37) Massiot, D.; Fayon, F.; Capron, M.; King, I.; Le Calvé, S.; Alonso, B.; Durand, J-O.; Bujoli, B.; Gan, Z.; Hoatson, G. *Magn. Reson. Chem.* **2002**, *40*, 70.

(38) Gaussian 03, Revisions B.04 and C.02, Frisch, M. J.; Trucks, G. W.; Schlegel, H. B.; Scuseria, G. E.; Robb, M. A.; Cheeseman, J. R.; Montgomery, Jr., J. A.; Vreven, T.; Kudin, K. N.; Burant, J. C.; Millam, J. M.; Iyengar, S. S.; Tomasi, J.; Barone, V.; Mennucci, B.; Cossi, M.; Scalmani, G.; Rega, N.; Petersson, G. A.; Nakatsuji, H.; Hada, M.; Ehara, M.; Toyota, K.; Fukuda, R.; Hasegawa, J.; Ishida, M.; Nakajima, T.; Honda, Y.; Kitao, O.; Nakai, H.; Klene, M.; Li, X.; Knox, J. E.; Hratchian, H. P.; Cross, J. B.; Bakken, V.; Adamo, C.; Jaramillo, J.; Gomperts, R.; Stratmann, R. E.; Yazyev, O.; Austin, A. J.; Cammi, R.; Pomelli, C.; Ochterski, J. W.; Ayala, P. Y.; Morokuma, K.; Voth, G. A.; Salvador, P.; Dannenberg, J. J.; Zakrzewski, V. G.; Dapprich, S.; Daniels, A. D.; Strain, M. C.; Farkas, O.; Malick, D. K.; Rabuck, A. D.; Raghavachari, K.; Foresman, J. B.; Ortiz, J. V.; Cui, Q.; Baboul, A. G.; Clifford, S.; Cioslowski, J.; Stefanov, B. B.; Liu, G.; Liashenko, A.; Piskorz, P.; Komaromi, I.; Martin, R. L.; Fox, D. J.; Keith, T.; Al-Laham, M. A.; Peng, C. Y.; Nanayakkara, A.; Challacombe, M.; Gill, P. M. W.; Johnson, B.; Chen, W.; Wong, M. W.; Gonzalez, C.; and Pople, J. A. *Gaussian, Inc., Wallingford CT*, **2004**.

(39) Dow, J.; Jensen, L. H.; Mazumdar, S. K.; Srinivasan, R.; Ramachandran, G. N. *Acta Crystallogr.* **1970**, *B26*, 1662.

(40) Takigawa, T.; Ashida, T.; Sasada, Y.; Kakudo, M. *Bull. Chem. Soc. Jpn.* **1966**, *39*, 2369.

(41) Bhaduri, D.; Saha, N. N. *J. Cryst. Mol. Struct.* **1979**, *9*, 311.

(42) Al-Karaghouli, A. R.; Koetzle, T. F. *Acta Crystallogr.* **1975**, *B31*, 2461.

(43) Al-Karaghouli, A. R.; Cole, F. E.; Lehmann, M. S.; Miskell, C. F.; Verbist, J. J.; Koetzle, T. F. *J. Chem. Phys.* **1975**, *63*, 1360.

(44) Koetzle, T. F.; Golic, L.; Lehmann, M. S.; Verbist, J. J.; Hamilton, W. C. *J. Chem. Phys.* **1974**, *60*, 4690.

(45) Sequeira, A.; Rajagopal, H.; Chidambaram, R. *Acta Crystallogr.* **1972**, *B28*, 2514.

(46) Frey, M. N.; Koetzle, T. F.; Lehmann, M. S.; Hamilton, W. C. *J. Chem. Phys.* **1973**, *58*, 2547.

(47) Becke, A. D. *J. Chem. Phys.* **1993**, *98*, 5648.

(48) (a) Perdew, J. P.; Burke, K.; Ernzerhof, M. *Phys. Rev. Lett.* **1996**, *77*, 3865. (b) Perdew, J. P.; Burke, K.; Ernzerhof, M. *Phys. Rev. Lett.* **1997**, *78*, 1396.

(49) Maseras, F.; Morokuma, K. *J. Comput. Chem.* **1995**, *16*, 1170.

(50) Dapprich, S.; Komáromi, I.; Byun, K. S.; Morokuma, K.; Frisch, M. J. *J. Mol. Struct. (Theochem)* **1999**, *462*, 1.

(51) Vreven, T.; Morokuma, K. *J. Comput. Chem.* **2000**, *21*, 1419.

(52) Vreven, T.; Byun, K. S.; Komáromi, I.; Dapprich, S.; Montgomery, J. A.; Morokuma, K.; Frisch, M. J. *J. Chem. Theory Comput.* **2006**, *2*, 815.

(53) Adiga, S.; Bryce, D. L. EFGShield, **2006**, University of Ottawa.

(54) Pyykkö, P. *Mol. Phys.* **2001**, *99*, 1617.

(55) Honda, H. *Z. Naturforsch.* **2003**, *58a*, 623.

(56) Bryce, D. L.; Gee, M.; Wasylishen, R. E. *J. Phys. Chem. A* **2001**, *105*, 10413.

(57) Mitsui, Y.; Tsuboi, M.; Iitaka, Y. *Acta Crystallogr.* **1969**, *B25*, 2182.